Metal Cation Complexation and Activation of Reversed CPyI Analogues of CC-1065 and Duocarmycin SA: Partitioning the Effects of Binding and Catalysis

David A. Ellis, Scott E. Wolkenberg, and Dale L. Boger*

Contribution from the Department of Chemistry and The Skaggs Institute for Chemical Biology, The Scripps Research Institute, 10550 North Torrey Pines Road, La Jolla, California 92037

Received March 23, 2001

Abstract: The synthesis and examination of a novel class of reversed CPyI analogues of CC-1065 and the duocarmycins are described. Capable of a unique metal cation activation of DNA alkylation, these agents allowed the effects of the DNA binding domain (10^4-fold increase in DNA alkylation rate and efficiency) to be partitioned into two components: that derived from enhanced DNA binding affinity and selectivity (10−80-fold) and that derived from a contribution to catalysis (250−5000-fold). In addition, the reversed enantiomeric selectivity of these sequence selective DNA alkylating agents provides further strong support for a previously disclosed model where it is the noncovalent binding selectivity of the compounds, and not the alkylation subunit or the source of catalysis, that controls the DNA alkylation selectivity.

Introduction

Duocarmycin SA (**1**)[1] and duocarmycin A (**2**)[2] constitute the parent members of a class of potent antitumor antibiotics[3] related to CC-1065 (**3**)[4] that derive their properties through a sequence selective alkylation of duplex DNA (Figure 1).[5−12] Since their disclosure, substantial efforts have been devoted to defining the characteristics of their DNA alkylation reactions, to determining the origin of their DNA alkylation selectivity, and to defining fundamental relationships between structure, functional reactivity, and biological properties.[5,6]

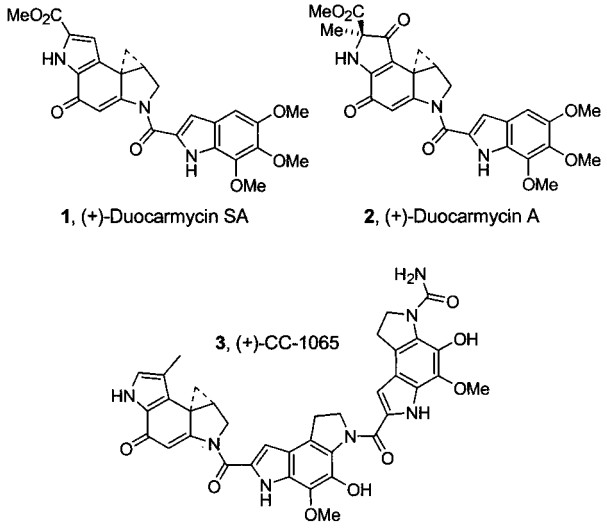

Figure 1.

Although unreactive toward conventional nucleophiles at pH 7, the DNA alkylation reactions by **1**−**3** are exceptionally facile, proceeding in <1 h at 4−25 °C. This latter reactivity is the result of catalysis that we have suggested is derived from a DNA binding-induced conformational change in the agents which activates them for nucleophilic attack.[13−15] This conformational change twists the linking amide and disrupts the vinylogous amide conjugation stabilizing the alkylation subunit. Because this conformational change is dependent upon the shape of the

(1) Ichimura, M.; Ogawa, T.; Takahashi, K.; Kobayashi, E.; Kawamoto, I.; Yasuzawa, T.; Takahashi, I.; Nakano, H. *J. Antibiot.* **1990**, *43*, 1037.

(2) Takahashi, I.; Takahashi, K.; Ichimura, M.; Morimoto, M.; Anaso, K.; Kawamoto, I.; Tomita, F.; Nakano, H. *J. Antibiot.* **1988**, *41*, 1915.

(3) Yasuzawa, T.; Muroi, K.; Ichimura, M.; Takahashi, I.; Ogawa, T.; Takahashi, K.; Sano, H.; Saitoh, Y. *Chem. Pharm. Bull.* **1995**, *43*, 378.

(4) Chidester, C. G.; Krueger, W. C.; Mizsak, S. A.; Duchamp, D. J.; Martin, D. G. *J. Am. Chem. Soc.* **1981**, *103*, 7629.

(5) Hurley, L. H.; Needham-VanDevanter, D. R. *Acc. Chem. Res.* **1986**, *19*, 230. Warpehoski, M. A.; Hurley, L. H. *Chem. Res. Toxicol.* **1988**, *1*, 315. Warpehoski, M. A. In *Advances in DNA Sequence Specific Agents*; Hurley, L. H., Ed.; JAI: Greenwich, CT, 1992; Vol. 1, p 217.

(6) Boger, D. L.; Johnson, D. S. *Angew. Chem., Int. Ed. Engl.* **1996**, *35*, 1439. Boger, D. L.; Johnson, D. S. *Proc. Natl. Acad. Sci. U.S.A.* **1995**, *92*, 3642. Boger, D. L. *Acc. Chem. Res.* **1995**, *28*, 20. Boger, D. L. In *Advances in Heterocyclic Natural Product Synthesis*; Pearson, W. H., Ed.; JAI: Greenwich, CT, 1992; Vol. 2, p 1. Boger, D. L. *Chemtracts: Org. Chem.* **1991**, *4*, 329.

(7) Boger, D. L.; Johnson, D. S.; Yun, W. *J. Am. Chem. Soc.* **1994**, *116*, 1635.

(8) Boger, D. L.; Yun, W. *J. Am. Chem. Soc.* **1993**, *115*, 9872.

(9) Boger, D. L.; Ishizaki, T.; Zarrinmayeh, H.; Munk, S. A.; Kitos, P. A.; Suntornwat, O. *J. Am. Chem. Soc.* **1990**, *112*, 8961. Boger, D. L.; Ishizaki, T.; Zarrinmayeh, H.; Kitos, P. A.; Suntornwat, O. *J. Org. Chem.* **1990**, *55*, 4499. Boger, D. L.; Ishizaki, T.; Zarrinmayeh, H. *J. Am. Chem. Soc.* **1991**, *113*, 6645. Boger, D. L.; Yun, W.; Terashima, S.; Fukuda, Y.; Nakatani, K.; Kitos, P. A.; Jin, Q. *Bioorg. Med. Chem. Lett.* **1992**, *2*, 759.

(10) Boger, D. L.; Johnson, D. S.; Yun, W.; Tarby, C. M. *Bioorg. Med. Chem.* **1994**, *2*, 115. Boger, D. L.; Coleman, R. S.; Invergo, B. J.; Sakya, S. M.; Ishizaki, T.; Munk, S. A.; Zarrinmayeh, H.; Kitos, P. A.; Thompson, S. C. *J. Am. Chem. Soc.* **1990**, *112*, 4623.

(11) Sugiyama, H.; Hosoda, M.; Saito, I.; Asai, A.; Saito, H. *Tetrahedron Lett.* **1990**, *31*, 7197. Sugiyama, H.; Ohmori, K.; Chan, K. L.; Hosoda, M.; Asai, A.; Saito, H.; Saito, I. *Tetrahedron Lett.* **1993**, *34*, 2179. Yamamoto, K.; Sugiyama, H.; Kawanishi, S. *Biochemistry* **1993**, *32*, 1059. Asai, A.; Nagamura, S.; Saito, H. *J. Am. Chem. Soc.* **1994**, *116*, 4171.

(12) Reynolds, V. L.; Molineux, I. J.; Kaplan, D. J.; Swenson, D. H.; Hurley, L. H. *Biochemistry* **1985**, *24*, 6228. Hurley, L. H.; Lee, C.-S.; McGovern, J. P.; Warpehoski, M. A.; Mitchell, M. A.; Kelly, R. C.; Aristoff, P. A. *Biochemistry* **1988**, *27*, 3886. Hurley, L. H.; Warpehoski, M. A.; Lee, C.-S.; McGovern, J. P.; Scahill, T. A.; Kelly, R. C.; Mitchell, M. A.; Wicnienski, N. A.; Gehard, I.; Johnson, P. D.; Bradford, V. S. *J. Am. Chem. Soc.* **1990**, *112*, 4633.

10.1021/ja010769r CCC: $20.00
Published on Web 08/30/2001

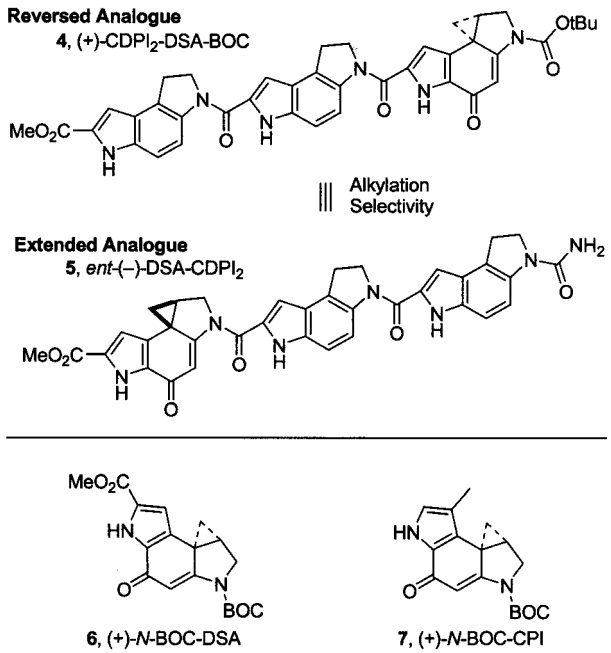

Figure 2.

minor groove and is greatest within the narrower, deeper AT-rich minor groove, this leads to preferential activation within the AT-rich noncovalent binding sites (shape-dependent catalysis).[14,15]

Insight into the source of catalysis for the DNA alkylation reaction was first described in the examination of reversed (**4**) versus extended (**5**) analogues of duocarmycin SA (Figure 2).[14] These studies established that the presence of the extended heteroaryl N^2 amide substituent conveys a special DNA alkylation reactivity that is independent of the alkylation sites and selectivity, and that the reversal of the orientation of the DNA binding subunits results in the complete reversal of the inherent enantiomeric DNA alkylation selectivity (Figure 2). Reversed analogues **4** displayed a substantial 100−1000-fold reduction in the rate of DNA alkylation, exhibiting rates similar to, but only 10-fold greater than, those of simple derivatives of alkylation subunits **6** and **7** themselves (Figure 2). We attributed the modest ~10-fold difference between the alkylation rates of **4** and **6** to the $CDPI_2$ enhancement of the DNA binding affinity of **4**,[16] whereas the larger 10^3-fold difference between **4** and **5** was attributed to the lack of binding-induced catalysis for **4** derived from disruption of the stabilizing vinylogous amide.

Recently, we reported the preparation of methyl 2-(*tert*-butyloxycarbonyl)-1,2,9,9a-tetrahydrocyclopropa[*c*]pyrido[3,2-*e*]indol-4-one-7-carboxylate (**8**, *N*-BOC-CPyI) (Figure 3).[17,18] Like **6** and **7**, it alkylates DNA with a rate and an efficiency that are approximately 10^4-fold lower than those for **1**−**3**. Unlike **6** and **7** or **1**−**3**, *N*-BOC-CPyI was capable of a metal cation initiated alkylation of DNA, and its 8-ketoquinoline structure

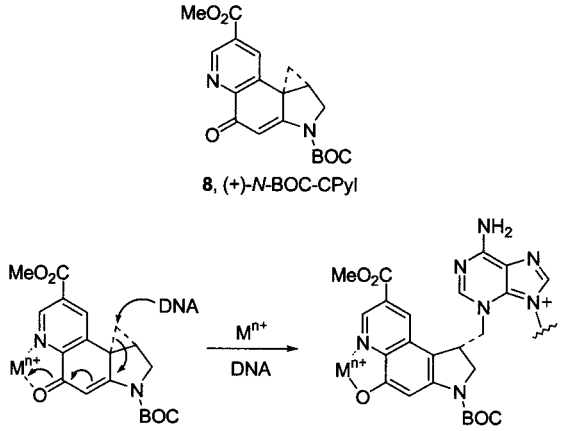

Figure 3.

provided a tunable means to effect activation via selective metal cation complexation ($Cu^{2+} > Ni^{2+} > Zn^{2+} > Cr^{2+} > Fe^{2+} > Mn^{2+} \gg Mg^{2+}$).[17−20] This activation was shown to promote an adenine N3 alkylation analogous to that observed with CC-1065 and the duocarmycins, and the efficiency of the DNA alkylation reaction of **8** was dramatically increased in the presence of Cu^{2+}, Ni^{2+}, and Zn^{2+}, the metal cations selected for detailed study.[19,20] This enhancement was as large as 1000-fold, was not observed for **6** and **7**, and resulted in no change in the DNA alkylation selectivity of **8**. Alkylation at such rates and low concentrations is unprecedented for such simple alkylation subunits and is within 10-fold of those of the natural products (+)-duocarmycin SA and (+)-CC-1065. In these studies, we suggested that the 1000-fold rate and efficiency enhancement was analogous to the 1000-fold catalysis contribution derived from the DNA binding domain attachment and that the remaining 10-fold difference in DNA alkylation efficiency may be attributed to differences in the noncovalent binding affinity due to the absence of an attached DNA binding subunit.[16] Thus, two independent studies showed that the DNA binding domain of **1**−**3** increases the DNA alkylation rate and efficiency 10^4-fold and indirectly deduced to do so by enhancing DNA binding affinity (~10-fold contribution) and contributing to catalysis (~10^3-fold).

Herein we disclose the synthesis and evaluation of **9**, a reversed analogue of duocarmycin SA containing the CPyI alkylation subunit that permits a more direct partitioning of the effects of binding and catalysis (Figure 4). Consistent with the proposal that the DNA alkylation sequence selectivity originates in the noncovalent binding selectivity of the agents and not the properties of the alkylation subunit itself, **9** exhibited the remarkable reversal of the inherent enantiomeric DNA alkylation selectivity characteristic of the reversed analogues: (+)-indole$_2$-CPyI-BOC = *ent*-(−)-CPyI-indole$_2$, and *ent*-(−)-indole$_2$-CPyI-BOC = (+)-CPyI-indole$_2$. This conforms nicely to past observations and models.[14] We also anticipated that **9** would be a poor DNA alkylating agent, but that the addition and chelation of metal cations would promote an efficient DNA alkylation. This provided an additional opportunity to examine the impact of the DNA binding domain on the rate and

(13) Boger, D. L.; Hertzog, D. L.; Bollinger, B.; Johnson, D. S.; Cai, H.; Goldberg, J.; Turnbull, P. *J. Am. Chem. Soc.* **1997**, *119*, 4977.

(14) Boger, D. L.; Bollinger, B.; Hertzog, D. L.; Johnson, D. S.; Cai, H.; Mésini, P.; Garbaccio, R. M.; Jin, Q.; Kitos, P. A. *J. Am. Chem. Soc.* **1997**, *119*, 4987.

(15) Boger, D. L.; Garbaccio, R. M. *Acc. Chem. Res.* **1999**, *32*, 1043.

(16) The AT-rich noncovalent binding affinities of compounds related to CC-1065 and the duocarmycins have been shown to increase incrementally with the addition of each subunit. See: Boger, D. L.; Coleman, R. S.; Invergo, B. J.; Zarrinmayeh, H.; Kitos, P. A.; Thompson, S. C.; Leong, T.; McLaughlin, L. W. *Chem.-Biol. Interact.* **1990**, *73*, 29. Review: Boger, D. L. In *Advances in Heterocyclic Natural Product Synthesis*; Pearson, W. H., Ed.; JAI: Greenwich, CT, 1992; Vol. 2, pp 1−188.

(17) Boger, D. L.; Boyce, C. W. *J. Org. Chem.* **2000**, *65*, 4088.

(18) Notably, all solution studies to date with all natural or analogue alkylation subunits exhibit clean S_N2, not S_N1, addition to the activated cyclopropane. In addition, the regioselectivity of nucleophilic addition to **8** (>20:1) favoring attack at the least substituted versus more substituted (most stable carbocation) cyclopropane carbon is further consistent with this expectation.

(19) Boger, D. L.; Wolkenberg, S. E.; Boyce, C. W. *J. Am. Chem. Soc.* **2000**, *122*, 6325.

(20) Throughout this paper, the acetylacetonate (acac) complex of the indicated metal cation was studied (e.g., Zn^{2+} refers to $Zn(acac)_2$).

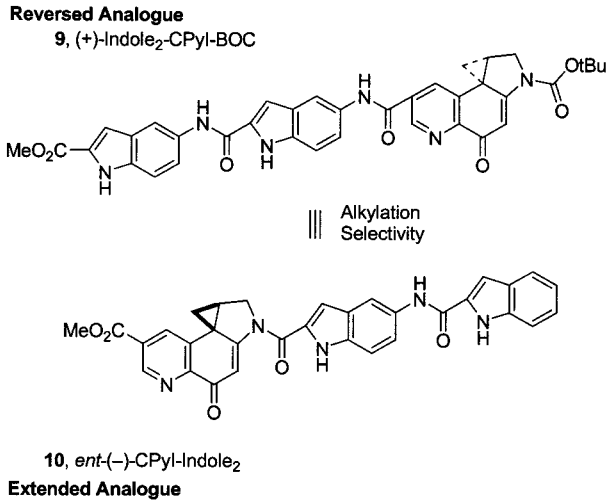

Figure 4.

efficiency of DNA alkylation (**9** versus **10**), partitioning it into measurable contributions derived from minor groove binding affinity versus catalysis.

Resolution of 11

To assess the properties of both enantiomers of the CPyI-based agents, direct chromatographic resolution of **11**[17] on a ChiralCel-OD semipreparative HPLC column (10 μm, 2 cm × 25 cm, 10% *i*-PrOH−hexanes, 8 mL/min, $\alpha = 1.16$) provided both enantiomers of this advanced intermediate (>99% ee), Scheme 1. The slower eluting (−)-enantiomer of **11** ($t_R = 42$ min) possesses the natural (3*S*)-configuration on the basis of its conversion to (+)-**8** and comparison with an authentic sample.[17] The reversed analogues derived from this enantiomer exhibit the more potent biological activity, the more effective DNA alkylation properties, and a DNA alkylation selectivity identical with that of the unnatural enantiomers of the natural products. The faster eluting (+)-enantiomer of **11** ($t_R = 36$ min) possesses the unnatural (3*R*)-configuration, correlated with *ent*-(−)-**8**,[17] and the reversed analogues derived from this enantiomer exhibit the corresponding less potent biological activity, the less effective DNA alkylation properties, and a DNA alkylation selectivity identical to that of the natural enantiomers of the natural products.

Synthesis of Indole$_2$-CPyI-BOC (9)

The preparation of the reversed analogue indole$_2$-CPyI-BOC (**9**) was accomplished through coupling of the free amine of **13** with the C7 carboxylic acid of **12** as outlined in Scheme 1. Hydrolysis of methyl ester **11** cleanly provided **12** (LiOH, 90%). Direct coupling of **12** with **13**[21] (1.1 equiv, 1.0 equiv of HOBt, 1.5 equiv of EDCI, 0.1 M DMF, 4−8 h, 25 °C) provided benzyl ether **14** in good yields (80−90%).[22] Two-phase, transfer catalytic hydrogenolysis[23] of **14** (Pd−C, 25 equiv of 25% aq HCO_2NH_4, THF, 25 °C, 3 h) afforded **15** (96%), and subsequent spirocyclization[24] was effected by treatment with DBU (1,8-diazabicyclo[4.3.0]undec-7-ene, DMF, 25 °C, 3 h) to provide **9** (67%).

Scheme 1

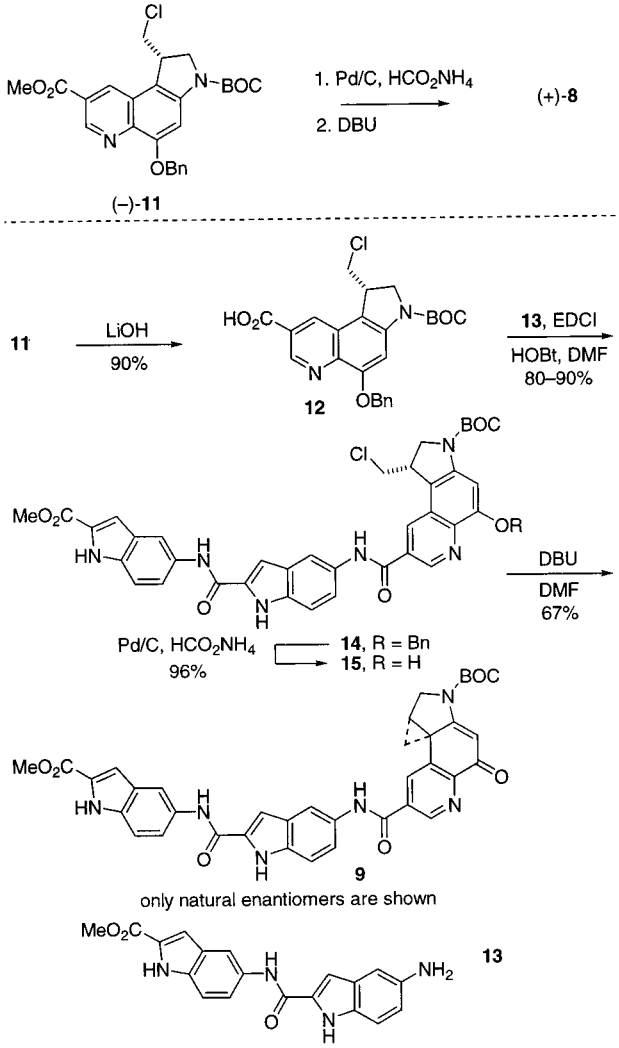

Modifications in the Terminal N^2 Acyl Substitutent of the Reversed Analogues

To ensure that the behavior of **9** was not substantially influenced by the nature of the N^2 substituent, both enantiomers of **16** and **19**, terminating with an N^2 free amine or an acetyl group, were also prepared (Scheme 2). Thus, *N*-BOC deprotection (4 N HCl/EtOAc, 25 °C, 30 min) of **15** followed by spirocyclization (saturated aq $NaHCO_3$, THF, 25 °C, 5 h) afforded **16** (81%). In a similar fashion, *N*-BOC deprotection of **14** followed by N^2 acetylation (CH_3COCl, 3 equiv of $NaHCO_3$, DMF) provided benzyl ether **17** (81%). Two-phase, catalytic transfer hydrogenolysis of **17** (Pd−C, 25 equiv of 25% aq HCO_2NH_4, 25 °C, 4 h) produced **18** (99%), and subsequent spirocyclization of **18** upon treatment with saturated aq $NaHCO_3$ in THF afforded **19** (92%).

DNA Alkylation Properties of Reversed versus Extended CPyI Analogues

The DNA alkylation properties were examined within w794 and its complement w836 DNA for which comparison results are available for related agents. The alkylation site identification and the assessment of the relative selectivity among the available sites were obtained by thermally induced strand cleavage of the singly 5'-end-labeled duplex DNA after exposure to the

(21) Boger, D. L.; Yun, W.; Han, N. *Bioorg. Med. Chem.* **1995**, *3*, 1429.

(22) Although straightforward as described in Scheme 1, initial attempts at coupling **12** with **13** (1.1 equiv, 3 equiv of EDCI, 0.05 M DMF, 12 h, 25 °C) were problematic. These conditions provided an acyl urea in good yield (62%) as a single regioisomer (structure confirmed by ^{1}H−^{1}H COSY) and only low yields of **14** (23%). EDCI = 1-(3-dimethylaminopropyl)-3-ethylcarbodiimide hydrochloride.

(23) Ram, S.; Ehrenkaufer, R. E. *Synthesis* **1988**, 91. Szeja, W. *Synthesis* **1985**, 76.

(24) Baird, R.; Winstein, S. *J. Am. Chem. Soc.* **1963**, *85*, 567. Baird, R.; Winstein, S. *J. Am. Chem. Soc.* **1962**, *84*, 788. Winstein, S.; Baird, R. *J. Am. Chem. Soc.* **1957**, *79*, 756.

Scheme 2

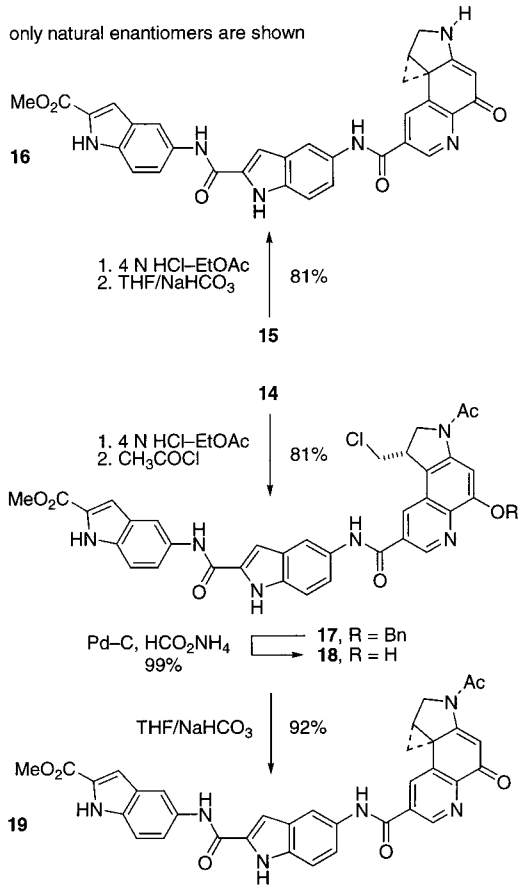

agents in 10 mM Tris buffer (pH 7.5). Following treatment of end-labeled duplex DNA with a range of agent and metal concentrations, the unbound agent was removed by ethanol precipitation of the DNA. Redissolution of the DNA in aqueous buffer, thermolysis (100 °C, 30 min) to induce strand cleavage at the sites of alkylation, denaturing polyacrylamide gel electrophoresis (PAGE) adjacent to Sanger sequencing lanes, and autoradiography led to identification of the DNA cleavage and alkylation sites. Full details of this procedure are included in the Supporting Information and have been disclosed elsewhere.[25]

A representative comparison of DNA alkylation by (+)-indole$_2$-CPyI-BOC (**9**) alongside duocarmycin SA and the extended analogues (+)- and *ent*-(−)-CPyI-indole$_2$ (**10**) within w794 is illustrated in Figure 5.[26,27] The natural enantiomer of the reversed agent (+)-indole$_2$-CPyI-BOC (**9**) was found to alkylate the same sites and to exhibit the same sequence selectivity as the unnatural enantiomer of duocarmycin SA and CPyI-indole$_2$ (**10**). This complete reversal of enantiomeric alkylation selectivity is only consistent with the noncovalent binding selectivity of the agents controlling the DNA alkylation sequence selectivity.[15] Thus, the natural enantiomer of reversed analogue (+)-indole$_2$-CPyI-BOC (**9**) alkylated the same, single high affinity site in w794 (5'AATTT) as the unnatural enantiomers (−)-duocarmycin SA and *ent*-(−)-CPyI-indole$_2$ (**10**) without detectable alkylation at the single high affinity site observed with the natural enantiomers (5'AATTA), Figure 5. Similar observations were made with unnatural enantiomer (−)-indole$_2$-CPyI-BOC (**9**) (Supporting Information, Figure S1). In addition to the reversal of the enantiomeric alkylation selectivities, the alkylation rates of the reversed analogues are much slower than those of duocarmycin SA and the extended agent

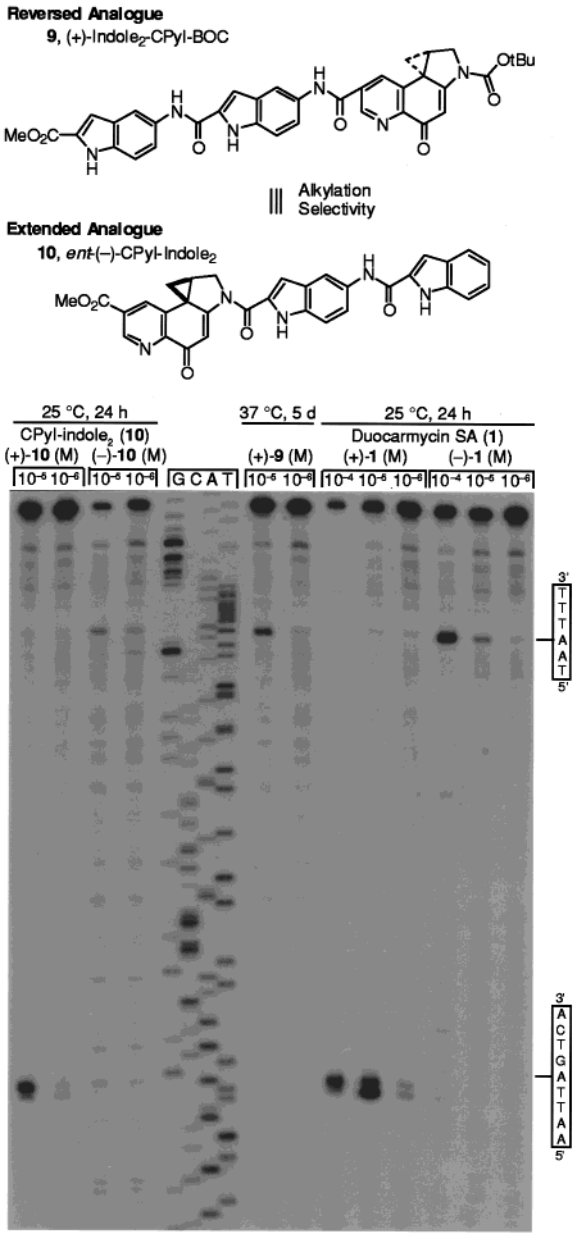

Figure 5. Thermally induced strand cleavage of w794 DNA (SV40 DNA segment, 144 bp, nucleotide nos. 138−5238); DNA-agent incubation at 25 °C (24 h, duocarmycin SA and CPyI-indole$_2$) or 37 °C (5 d, indole$_2$-CPyI-BOC), removal of unbound agent and 30 min of thermolysis (100 °C), followed by denaturing 8% PAGE and autoradiography. Lanes 1−2, (+)-CPyI-indole$_2$ (**10**, 1×10^{-5} and 1×10^{-6} M); lanes 3−4, (−)-CPyI-indole$_2$ (**10**, 1×10^{-5} and 1×10^{-6} M); lanes 5−8, Sanger G, C, A, and T sequencing reactions; lanes 9−10, (+)-indole$_2$-CPyI-BOC (**9**, 1×10^{-5} to 1×10^{-6} M); lanes 11−13, (+)-duocarmycin SA (**1**, 1×10^{-4} to 1×10^{-6} M); lanes 14−16, (−)-duocarmycin SA (**1**, 1×10^{-4} to 1×10^{-6} M). See Supporting Information for experimental details.

(25) Boger, D. L.; Munk, S. A.; Zarrinmayeh, H.; Ishizaki, T.; Haught, J.; Bina, M. *Tetrahedron* **1991**, *47*, 2661.

(26) The CPyI analogues **9** and **10** alkylate the same sites as **4** and **5**. See ref 13 for published comparison gel figures of **4** and **5** and a complete assessment of the selectivity. Only subtle distinctions analogous to prior indole$_2$ versus CDPI$_2$ relative alkylation efficiencies among available sites were observed.

(27) The concentrations listed in the figures for the compounds are those at which they were added to the DNA incubation solution where they are diluted a further 10-fold. The Zn(acac)$_2$ concentrations are reported in the figures as equivalents. Thus, the Figure 6 concentrations of Zn(acac)$_2$ resulting in catalysis are 100 μM (lanes 16 and 18) and 1 mM (lanes 19 and 20). The Figure 7 concentrations of Zn(acac)$_2$ resulting in catalysis are 100 μM (lane 14), 1 mM (lane 15 and 17), and 10 mM (lane 16 and 18).

Table 1. Relative Rates of DNA Alkylation

compound	relative rate[a]	k_{rel} (nat/unnat)	k_{rel} (nat)	k_{rel} (unnat)
10, (+)-CPyI-indole$_2$	1		620 (20 700)	
9, (+)-indole$_2$-CPyI-BOC	0.0016	7	1 (33)	
9, (−)-indole$_2$-CPyI-BOC	0.000 24			1
19, (+)-indole$_2$-CPyI-Ac	0.0040	3	2.5 (83)	
19, (−)-indole$_2$-CPyI-Ac	0.0013			5
16, (+)-indole$_2$-CPyI-H	0.000 61	3	0.4 (13)	
16, (−)-indole$_2$-CPyI-H	0.000 20			0.8
8, (+)-*N*-BOC-CPyI	0.000 05		0.03 (1)	
8, (+)-*N*-BOC-CPyI + Zn^{2+}	0.011		6.9 (230)	
9, (+)-indole$_2$-CPyI-BOC + Zn^{2+}	1.4		857 (28 600)	

[a] Averaged relative rates of DNA alkylation within w794 and its complement w836, four experiments averaged. See Supporting Information for experimental details including absolute rate constants.

CPyI-indole$_2$. Whereas alkylation is observed at concentrations as low as 10^{-5} M with *ent*-(−)-duocarmycin SA and 10^{-6} M with (+)-duocarmycin SA after incubation at room temperature for 24 h, alkylation at similar concentrations of indole$_2$-CPyI-BOC (**9**) requires much more vigorous conditions (5 d, 37 °C, Figure 5) proceeding at a rate that is approximately 1000-fold slower (see Table 1).

The simple derivative *N*-BOC-CPyI (**8**), behaves analogously to simple alkylation subunit derivatives of duocarmycin SA (**6**, *N*-BOC-DSA) and analogues (e.g., *N*-BOC-CBI) in the absence of metal cations (alkylation at $10^{-2}-10^{-3}$ M, 24 h, 25 °C), Figure 6.[27] In addition, this characteristic alkylation selectivity of the simple alkylation subunit derivatives is independent of the absolute stereochemistry with both enantiomers alkylating the same sites and is considerably less selective than that of the natural products or the extended and reversed analogues.[5−12] In the presence of the metal cations selected for study (Cu^{2+}, Ni^{2+}, and Zn^{2+}), the alkylation efficiency of **8**, but not **6** or **7**, increased without altering the characteristic alkylation selectivity.[19] This indicates that the source of the alkylation selectivity for **8** (**6**−**8**) is not uniquely embedded in the catalysis source, which is consistent with proposals that it is derived from the compound's noncovalent binding selectivity. The enhancement was most pronounced with Zn^{2+}, which increased the efficiency 1000-fold such that alkylation is observed at 10^{-5} M versus 10^{-2} M (24 h, 25 °C, Figure 6). Zinc cations have been shown to bind DNA and alter its structure,[28] and it is possible that these effects are responsible for the enhanced DNA alkylation rate and efficiency of **8** in the presence of Zn(acac)$_2$. However, the absence of any effect on the behavior of **6**, **7**, CC-1065, or duocarmycin SA,[19] and the observation that the sequence selectivity of **8** (or **9**) is unaltered in the presence of Zn(acac)$_2$ suggest this is unlikely.

Representative results of analogous studies with the reversed CPyI analogues are illustrated in Figure 7.[27] After incubation with w794 DNA for 24 h at 25 °C, (+)-indole$_2$-CPyI-BOC (**9**) alkylates the high affinity site for (−)-duocarmycin SA at concentrations as low as 10^{-4} M. This corresponds to an increase in alkylation rate and efficiency over the simple *N*-BOC-CPyI derivative (alkylation at $10^{-2}-10^{-3}$ M) of ∼10−50-fold, and we attribute this increase to the enhanced noncovalent binding of **9** derived from the attached indole$_2$ DNA binding subunit.[16]

(28) (a) Gueron, M.; Weisbuch, G. *Biochimie* **1981**, *63*, 821. Marzilli, L. G.; Kistenmacher, T. J. *Acc. Chem. Res.* **1977**, *10*, 146. (b) Although Zn^{2+} complexes with adenine have been characterized (N7/N9)[28c] and inferred within DNA,[28d] the association constants are very weak[28e] and Zn^{2+} is principally associated with the phosphate backbone.[28d] (c) Srinivasan, L.; Taylor, M. R. *J. Chem. Soc., Chem. Commun.* **1970**, 1668. (d) Shin, Y. A.; Eichhorn, G. L. *Biochemistry* **1968**, *7*, 1026. (e) Wang, S. M.; Li, N. C. *J. Am. Chem. Soc.* **1968**, *90*, 5069.

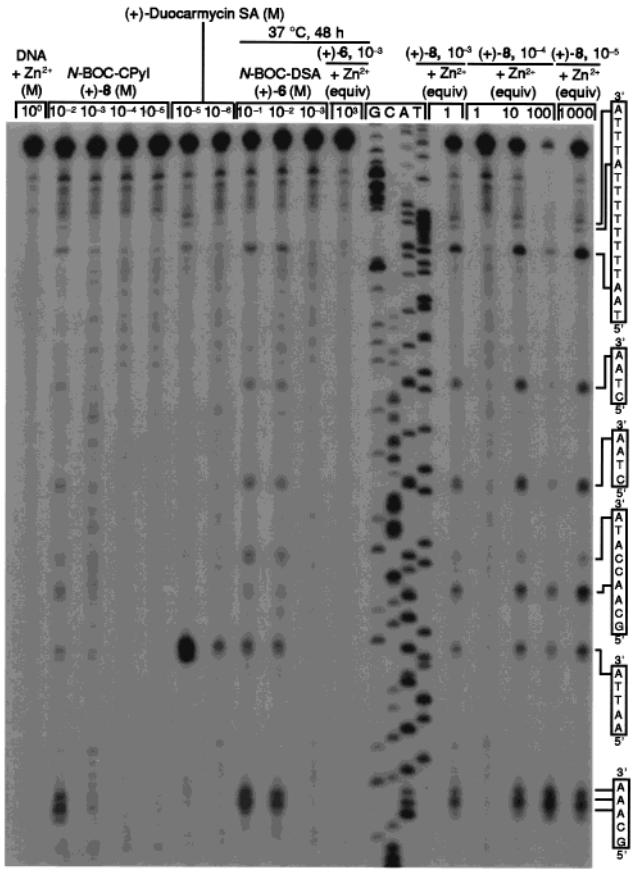

Figure 6. Thermally induced strand cleavage of w794 DNA (SV40 DNA segment, 144 bp, nucleotide nos. 138−5238); DNA-agent incubation at 25 °C (24 h, duocarmycin SA and *N*-BOC-CPyI) or 37 °C (48 h, *N*-BOC-DSA), removal of unbound agent and 30 min of thermolysis (100 °C), followed by denaturing 8% PAGE and autoradiography. Lane 1, control DNA with Zn(acac)$_2$ (1×10^0 M); lanes 2−5, (+)-*N*-BOC-CPyI (**8**, 1×10^{-2} to 1×10^{-5} M); lanes 6−7, (+)-duocarmycin SA (1×10^{-5} and 1×10^{-6} M); lanes 8−10, (+)-*N*-BOC-DSA (**6**, 1×10^{-1} to 1×10^{-3} M); lane 11, (+)-*N*-BOC-DSA (**6**, 1×10^{-3} M) with Zn(acac)$_2$ (1000 equiv); lanes 12−15, Sanger G, C, A, and T sequencing reactions; lane 16, (+)-*N*-BOC-CPyI (**8**, 1×10^{-3} M) with Zn(acac)$_2$ (1 equiv); lanes 17−19, (+)-*N*-BOC-CPyI (**8**, 1×10^{-4} M) with Zn(acac)$_2$ (1, 10, and 100 equiv); lane 20, (+)-*N*-BOC-CPyI (**8**, 1×10^{-5} M) with Zn(acac)$_2$ (1000 equiv). See Supporting Information for experimental details.

An increase in DNA alkylation rate and efficiency of **9** is observed upon the addition of Cu^{2+}, Ni^{2+}, or Zn^{2+}. Without altering the sequence selectivity, the addition of each of these metal cations increases the alkylation efficiency to a level comparable to that of the natural product and extended agents, with alkylation by **9** observed at concentrations as low as 10^{-6} M (25 °C, 24 h, data for Cu^{2+} and Ni^{2+} not shown), Figure 7. An analogous 100-fold increase in the efficiency of DNA alkylation by the unnatural enantiomer of **9** is illustrated in the Supporting Information (Figure S1). Not only does this indicate that the characteristic alkylation selectivity is independent of the source of catalysis, but these results enable us to partition the effects of the DNA alkylation efficiency at an arbitrary time point in a semiquantitative fashion. The alkylation subunit alone (**8**, *N*-BOC-CPyI) provides a baseline inherent rate and efficiency with alkylation observed at concentrations of $10^{-2}-10^{-3}$ M (25 °C, 24 h). The addition of a DNA binding subunit without the addition of activation features (i.e., the reversed analogues) results in a 10−50-fold increase in rate and efficiency (**9** alkylates DNA at concentrations as low as 10^{-4} M after 24 h at 25 °C).

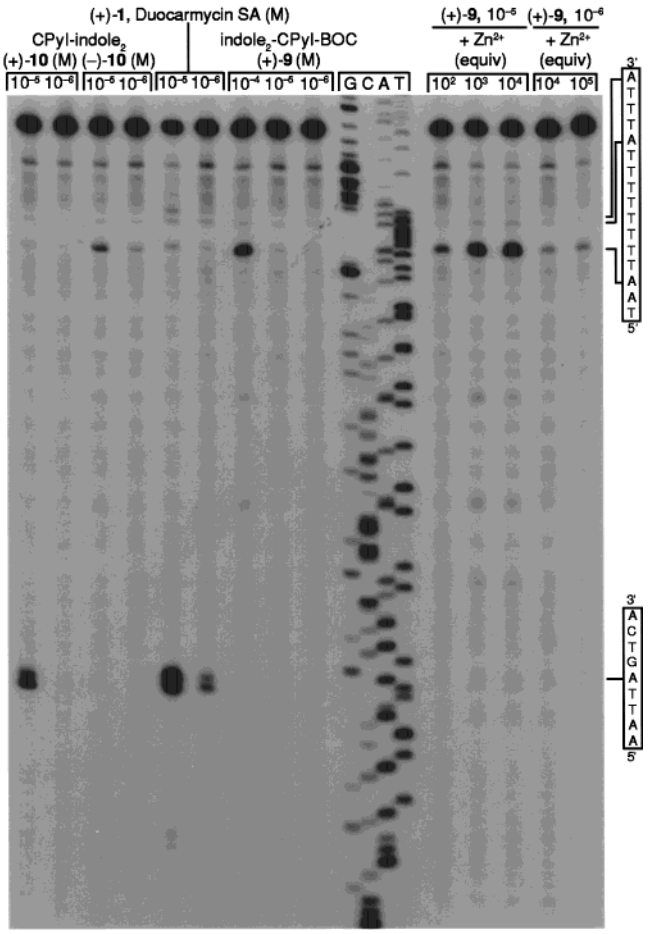

Figure 7. Thermally induced strand cleavage of w794 DNA (SV40 DNA segment, 144 bp, nucleotide nos. 138−5238); DNA-agent incubation at 25 °C for 24 h, removal of unbound agent and 30 min of thermolysis (100 °C), followed by denaturing 8% PAGE and autoradiography. Lanes 1−2, (+)-CPyI-indole$_2$ (**10**, 1×10^{-5} and 1×10^{-6} M); lanes 3−4, (−)-CPyI-indole$_2$ (**10**, 1×10^{-5} and 1×10^{-6} M); lanes 5−6, (+)-duocarmycin SA (**1**, 1×10^{-5} and 1×10^{-6} M); lanes 7−9, (+)-indole$_2$-CPyI-BOC (**9**, 1×10^{-4} to 1×10^{-6} M); lanes 10−13, Sanger G, C, A, and T sequencing reactions; lanes 14−16, (+)-indole$_2$-CPyI-BOC (**9**, 1×10^{-5} M) with Zn(acac)$_2$ (100, 1000, and 10^4 equiv); lanes 17−18, (+)-indole$_2$-CPyI-BOC (**9**, 1×10^{-6} M) with Zn(acac)$_2$ (10^4 and 10^5 equiv). See Supporting Information for experimental details.

In previous studies,[13−15] the remaining difference between the natural products and the reversed analogues was attributed to activation toward nucleophilic attack provided by the binding-induced twist in the linking amide disrupting the vinylogous amide stabilization present only in the natural products and their extended analogues. With the alternative metal cation activation available to CPyI, it is possible to directly observe such a catalysis contribution to the DNA alkylation efficiency. This direct observation corresponds beautifully to previous estimates (∼100-fold). Thus, with the reversed CPyI analogues in the presence of Zn^{2+}, the noncovalent binding contribution (10−50-fold) and catalysis contribution provided by the metal cation (∼100-fold) at an arbitrary time point combine to provide an efficiency equal to that of the natural products. A more careful characterization of the relative rates versus eventual efficiency of DNA alkylation is summarized in the next section.

DNA Alkylation Properties of Reversed CPyI Analogues Containing Modifications in the Terminal N^2 Substituent

Analogues **16** and **19** were examined in efforts to further establish whether the terminal N^2-BOC group of **9** was contributing significantly to its reduced rate and efficiency of DNA alkylation (Table 1). The three agents exhibited no differences in their DNA alkylation selectivity, only small differences in the rate and efficiency of their DNA alkylation, and all were orders of magnitude less effective than the natural products or typical extended analogues including CPyI-indole$_2$ (**10**). The distinctions were especially clear when comparing the relative rates of DNA alkylation (Table 1). Relative to the extended analogue (+)-CPyI-indole$_2$ (**10**), the reversed analogues were approximately 1000-fold slower at alkylating DNA (250−5000 times). The natural enantiomers of the reversed CPyI analogues were only 10−80 times faster at alkylating DNA than (+)-*N*-BOC-CPyI, which lacks a DNA binding subunit altogether. Of these comparisons, that of **8** and **9** (BOC derivatives) is most relevant, indicating that the attached DNA binding subunit of **9** increases the rate of DNA alkylation 33-fold. The natural enantiomers of the reversed analogues were 3−7 times faster at alkylating DNA than the corresponding unnatural enantiomers. Consistent with prior observations, the relative rates follow the order **19** > **9** > **16** (Ac > BOC > H), following trends expected on the basis of the relative reactivity of the compounds, but the differences are small relative to the behavior of traditional extended agents such as **10**. These observations confirmed that the nature of the simple N^2 substituent does not contribute significantly to the distinctions in the rate and alkylation efficiency observed with the reversed analogues.

Although less pronounced, these slower DNA alkylation rates also correlate with an overall lower efficiency of DNA alkylation. That is, prolonged reactions under vigorous conditions (37 °C, 5 d) provide overall DNA alkylation efficiencies that follow the rate trends (**19** > **9** > **16**), but more closely approach the final efficiencies of the natural products or their typical extended analogues. Acetyl derivative **19** was found to be approximately 2.5−5-fold more efficient than the N^2−BOC derivative, and the terminal N^2−H agent was about an order of magnitude less efficient than **19**. Artificially catalyzing the reaction of **9**, **16**, or **19** with the addition of Zn^{2+} provides efficiencies of DNA alkylation that are not distinguishable from those of the natural products or their extended analogues, whereas those of **8** are only a remarkably 10-fold lower.

Table 2. Cytotoxic Activity, L1210 IC$_{50}$ (pM)

natural enantiomer	IC$_{50}$	unnatural enantiomer	IC$_{50}$
10, (+)-CPyI-indole$_2$	8	**10**, (−)-CPyI-indole$_2$	45
9, (+)-indole$_2$-CPyI-BOC	1300	**9**, (−)-indole$_2$-CPyI-BOC	3800
19, (+)-indole$_2$-CPyI-Ac	800	**19**, (−)-indole$_2$-CPyI-Ac	1200
16, (+)-indole$_2$-CPyI-H	9600	**16**, (−)-indole$_2$-CPyI-H	13 000
8, (+)-*N*-BOC-CPyI	110 000	**8**, (−)-*N*-BOC-CPyI	70 000

Cytotoxic Activity

The cytotoxic potencies of the reversed analogues are summarized in Table 2. Their trends parallel those made in the DNA alkylation studies. The natural enantiomers of the reversed analogues were 100−1000 times less potent than the typical extended analogue (+)-CPyI-indole$_2$ (**10**) and only 10−100 times more potent than the simple derivative *N*-BOC-CPyI (**8**), which lacks a DNA binding subunit. The natural enantiomers of the reversed analogues were consistently, but only slightly (∼1.5−3 times), more potent than the corresponding unnatural enantiomers, whereas the differences among the extended analogues of CPyI were typically larger (3−30-fold, 5−6 times for **10**).[17] The nature of the terminal N^2 substituent of the reversed analogues does influence the cytotoxic potency (Ac > BOC > H) with magnitudes in the trends that mirror those

observed in the relative efficiencies of DNA alkylation, but these differences are small relative to the comparisons with **10**. Finally, the seco precursors **15** and **18** exhibited cytotoxic potencies indistinguishable from those of the cyclopropane containing compounds.

Discussion and Conclusions

The preparation and examination of a novel class of reversed CPyI analogues of CC-1065 and the duocarmycins that are capable of a tunable metal cation catalyzed DNA alkylation reaction were described. The reversed enantiomeric selectivity of the DNA alkylation reaction by the analogues indicate that it is not the alkylation subunit that controls the alkylation selectivity, but rather the noncovalent binding selectivity of the compounds that controls the sites of DNA alkylation. Moreover, this DNA alkylation reaction proved to be subject to metal cation activation, increasing both the rate and efficiency of DNA alkylation without affecting the inherent DNA alkylation selectivity. Thus, the alkylation selectivity does not appear to be uniquely embedded in the catalysis source, consistent with proposals that it is derived from the noncovalent binding selectivity. Even more importantly, the reversed CPyI analogues provide the opportunity to probe the role of the DNA binding subunits which in recent studies has been suggested to extend beyond that of simply providing DNA binding affinity and selectivity by contributing to catalysis as well. The comparison of the rates of DNA alkylation by the reversed CPyI analogues, *N*-BOC-CPyI, and the typical extended analogue CPyI-indole$_2$ permitted the partitioning of the effects of DNA binding subunits (21 000-fold) into that derived from increased binding affinity and selectivity (33-fold) and that derived from a contribution to catalysis (620-fold). Thus, the rate difference observed between the reversed CPyI analogues and *N*-BOC-CPyI indicate that the DNA binding subunits binding affinity and selectivity increase the rate of DNA alkylation 33-fold. The comparison of CPyI-indole$_2$ and the reversed CPyI analogues indicates the DNA binding subunits' larger contribution to catalysis is 250−5000-fold (620-fold for BOC derivative), a contribution that we suggest is due to a DNA binding-induced conformational change that disrupts the stabilizing vinylogous amide conjugation. With the reversed CPyI analogues, addition of the metal cation Zn^{2+} artificially replaced this inaccessible source of catalysis, providing rates and efficiencies of DNA alkylation that were not distinguishable from those of the natural products or typical extended analogues without affecting the alkylation selectivity. Moreover, this complementary measure of the contributions of binding and catalysis to the alkylation rate available to CPyI analogues provided remarkably similar results. For contributions attributable to binding, comparisons give values of 33-fold ((+)-*N*-BOC-CPyI vs (+)-indole$_2$-CPyI-BOC) and 90-fold ((+)-*N*-BOC-CPyI + Zn^{2+} vs (+)-CPyI-indole$_2$). For contributions attributable to catalysis, comparisons give values of 620-fold ((+)-indole$_2$-CPyI-BOC vs (+)-CPyI-indole$_2$), 860-fold ((+)-indole$_2$-CPyI-BOC vs (+)-indole$_2$-CPyI-BOC + Zn^{2+}), and 230-fold ((+)-*N*-BOC-CPyI vs (+)-*N*-BOC-CPyI + Zn^{2+}). Similarly, the modest 10-fold difference in DNA alkylation efficiency between the natural products or typical extended CPyI analogues and the simple *N*-BOC-CPyI alkylation subunit **8** in the presence of Zn^{2+} indicates that the noncovalent minor groove binding of the full agents and proximity effects imposed on these DNA-bound agents contribute less to the overall DNA alkylation efficiency than previously believed. Instead, the larger, additional, approximately 1000-fold contribution of the DNA binding subunits to DNA alkylation efficiency within this family of compounds may be attributed to catalysis which we suggest is derived through a DNA-binding induced twist in the linking N^2 amide which disrupts the vinylogous amide stabilization of the alkylation subunit and increases their reactivity toward nucleophilic attack.

Finally, although there are several well-established methods available for selective activation[29] of DNA binding agents, including reductive activation (mitomycins), oxidative activation (aflatoxin), disulfide or trisulfide cleavage (calicheamicin), photochemical activation (psoralen), and oxidant activation of metal complexes (bleomycin), we are not aware of examples of metal cation Lewis acid activation of a sequence selective DNA alkylating agent.[30] Many of these methods have been exploited in the development of therapeutics to impart selective activation against tumor cells. Thus, indole$_2$-CPyI-BOC (**9**) and related reversed CPyI analogues may have unique therapeutic applications. Comparative trace metal analyses of cancerous and noncancerous human tissue have revealed significant distinctions.[31] Although no generalizations were possible across all tumor types, within a given tumor type there were significant and potentially exploitable differences. For example, Zn was found in breast carcinoma at levels 700% higher than normal breast cells of the same type while lung carcinoma exhibited a reversed and even larger 10-fold difference.[31] Thus, chemotherapeutic agents subject to Zn activation might exhibit an enhanced activity against breast carcinoma attributable to this difference in Zn levels.[31] The results of the examination of these and related applications will be disclosed in due course.[32,33]

Experimental Section

5-(Benzyloxy)-3-(*tert*-butyloxycarbonyl)-1-(chloromethyl)-1,2-dihydro-3*H*-pyrido[3,2-*e*]indole-8-carboxylic Acid (12). A solution of **11**[17] (3.0 mg, 6.2 μmol) in THF/CH_3OH/H_2O (3:2:1, 130 μL) was cooled to 0 °C in an ice−water bath and treated with 21 μL of aq 3 N LiOH (10 equiv). The cooling bath was removed, and the solution was stirred at 25 °C for 3 h. The reaction mixture was quenched with the addition of aq 1 N $KHSO_4$ (62 μL, 1 equiv), diluted with H_2O (1 mL), and extracted with EtOAc (3 × 1 mL). The combined organic phase was dried (Na_2SO_4), filtered, and concentrated in vacuo. Chromatography (SiO_2, 0.7 cm × 6 cm, 5% CH_3OH−$CHCl_3$) afforded **12** (2.6 mg, 90%) as a light yellow film: ^{1}H NMR (DMF-d_7, 400 MHz) δ 9.32 (d, J = 1.7 Hz, 1H), 8.68 (d, J = 1.4 Hz, 1H), 8.10 (br s, 1H, obscured by DMF), 7.65 (apparent d, J = 7.2 Hz, 2H), 7.44 (t, J = 6.9 Hz, 2H), 7.38 (apparent t, J = 7.5 Hz, 1H), 5.38 (m, 2H), 4.23 (m, 3H), 4.06 (d, J = 10 Hz, 1H), 3.89 (m, 1H), 1.60 (s, 9H); IR (film) ν_{max} 3402, 2977, 2926, 1713, 1682 cm^{-1}; MALDI-HRMS (dihydroxybenzyl alcohol, DHB) m/z 469.1537 (M + H$^+$, $C_{25}H_{25}ClN_2O_5$ requires m/z 469.1530). (−)-(1*S*)-**12**: $[\alpha]^{25}_D$ −10 (*c* 0.1, DMF). *ent*-(+)-(1*R*)-**12**: $[\alpha]^{25}_D$ +9 (*c* 0.08, DMF).

***N*-(2-(*N*-((2-Methoxycarbonyl)indol-5-yl)carbamoyl)indol-5-yl)-5-(benzyloxy)-1-(chloromethyl)-3-(*tert*-butyloxycarbonyl)-1,2-dihydro-3*H*-pyrido[3,2-*e*]indole-8-carboxamide (14).** A solution of **12** (3.0 mg, 6.4 μmol, 1 equiv) and **13** (2.7 mg, 7.7 μmol, 1.2 equiv) in 60 μL of anhydrous DMF under Ar was treated sequentially with HOBt (0.9

(29) *Molecular Aspects of Anticancer Drug−DNA Ineractions*; Neidle, S., Waring, M., Eds.; CRC: Boca Raton, FL, 1993 and 1994; Vol. 1 and 2.

(30) A reviewer brought two less obvious examples of metal cation assisted DNA alkylations to our attention: Li, T.; Rokita, S. E. *J. Am. Chem. Soc.* **1991**, *113*, 7771. Hix, S.; Augusto, O. *Chem.-Biol. Interact.* **1999**, *118*, 141.

(31) Mulay, I. L.; Roy, R.; Knox, B. E.; Suhr, N. H.; Delaney, W. E. *J. Natl. Cancer. Inst.* **1971**, *47*, 1.

(32) The endogenous concentrations of zinc range from 25 to 1 μM with concentrations in some tissue being much higher, including the liver, gastrointestinal tract, skin, kidney, brain, and prostrate (5−10 mM).[33] Wastney, M. E.; Rennert, O. M.; Subramanian, K. N. S. In *Encyclopedia of Human Biology*, 2nd Ed.; Academic: San Diego, 1997; Vol. 8, p 791.

(33) Untergasser, G.; Rumpold, H.; Plas, E.; Witkowski, M.; Pfister, G.; Berger, P. *Biochem. Biophys. Res. Commun.* **2000**, *279*, 607.

mg, 6.4 μmol, 1 equiv) and EDCI (1.8 mg, 9.6 μmol, 1.5 equiv). The reaction mixture was stirred for 12 h at 25 °C before the solvent was removed under a stream of N_2. Chromatography (0.7 cm × 6 cm, SiO_2, 30:1 $CHCl_3/CH_3OH$) afforded **14** (3.9 mg, 80%) as a light yellow film: ^{1}H NMR (DMF-d_7, 400 MHz) δ 11.90 (s, 1H), 11.86 (s, 1H), 10.61 (s, 1H) 10.36 (s, 1H), 9.29 (d, J = 2.0 Hz, 1H), 9.02 (d, J = 1.7 Hz, 1H), 8.35 (m, 2H), 7.76 (dd, J = 2.0, 8.9 Hz, 1H), 7.67 (m, 2H), 7.64 (d, J = 1.7 Hz, 1H), 7.61 (s, 1H), 7.54 (m, 2H), 7.45 (t, J = 7.2 Hz, 2H), 7.40 (t, J = 7.5 Hz, 1H), 7.22 (d, J = 1.4 Hz, 1H), 5.43 (s, 2H), 4.27 (m, 4H), 4.02 (dd, J = 6.8, 11.0 Hz, 1H), 3.92 (s, 3H), 1.61 (s, 9H); IR (film) ν_{max} 3324, 2927, 1694, 1645 cm^{-1}; MALDI-HRMS (DHB) *m/z* 799.2663 (M + H$^+$, $C_{44}H_{39}ClN_6O_7$ requires *m/z* 799.2647). (+)-(1*S*)-**14**: $[\alpha]^{25}_D$ +22 (*c* 0.06, acetone). *ent*-(−)-(1*R*)-**14**: $[\alpha]^{25}_D$ −20 (*c* 0.055, acetone).

***N*-(2-(*N*-((2-Methoxycarbonyl)indol-5-yl)carbamoyl)indol-5-yl)-1-(chloromethyl)-5-hydroxy-3-(*tert*-butyloxycarbonyl)-1,2-dihydro-3*H*-pyrido[3,2-*e*]indole-8-carboxamide (15).** A suspension of **14** (3.2 mg, 4.0 μmol) and 10% Pd−C (3.2 mg, 1 wt equiv) in 80 μL of degassed, anhydrous THF was treated with 25% aq HCO_2NH_4 (6.3 mg, 25 μL, 100 μmol, 25 equiv). The reaction mixture was stirred for 3 h and filtered through a small plug of Celite. The filtrate was concentrated under a stream of N_2 to afford **15** (2.7 mg, 96%) as a light yellow film: ^{1}H NMR (DMF-d_7, 250 MHz) δ 11.91 (d, J = 2.1 Hz, 1H), 11.80 (s, 1H), 10.57 (s, 1H), 10.31 (s, 1H), 10.21 (br s, 1H), 9.22 (d, J = 2.1 Hz, 1H), 9.01 (d, J = 2.1 Hz, 1H), 8.35 (m, 2H), 8.04 (br s, 1H, obscured by DMF), 7.78 (dd, J = 1.6, 8.9 Hz, 1H), 7.63 (m, 2H), 7.56 (m, 2H), 7.23 (d, J = 2.1 Hz, 1H), 4.24 (m, 5H), 3.92 (s, 3H), 1.60 (s, 9H); IR (film) ν_{max} 3271, 2916, 2848, 1712, 1644 cm^{-1}; MALDI-HRMS (DHB) *m/z* 709.2189 (M + H$^+$, $C_{37}H_{33}ClN_6O_7$ requires *m/z* 709.2177). (−)-(1*S*)-**15**: $[\alpha]^{25}_D$ −110 (*c* 0.009, DMF). *ent*-(+)-(1*R*)-**15**: $[\alpha]^{25}_D$ +120 (*c* 0.009, DMF).

***N*-(2-(*N*-((2-Methoxycarbonyl)indol-5-yl)carbamoyl)indol-5-yl)-3-(*tert*-butyloxycarbonyl)-1,2,9,9a-tetrahydrocyclopropa[*c*]pyrido-[3,2-*e*]indol-4-one-7-carboxamide (Indole$_2$-CPyI-BOC, 9).** A solution of **15** (1.3 mg, 1.8 μmol) in 100 μL of anhydrous DMF under Ar was treated with DBU (0.82 mg, 5.4 μmol, 3 equiv). The reaction mixture was stirred for 3 h at 25 °C before the reaction mixture was directly subjected to flash chromatography (0.7 cm × 6 cm, SiO_2, 20% CH_2Cl_2−DMF) to afford **9** (0.8 mg, 67%) as a light yellow film: ^{1}H NMR (DMF-d_7, 250 MHz) δ 11.91 (s, 1H), 11.81 (s, 1H), 10.51 (s, 1H), 10.32 (s, 1H), 9.26 (d, J = 1.6 Hz, 1H), 8.34 (s, 1H), 8.32 (s, 1H), 8.27 (d, J = 2.1 Hz, 1H), 7.74 (dd, J = 1.6, 9 Hz, 1H), 7.61 (br s, 2H), 7.55 (m, 2H), 7.22 (d, J = 2.1, 1H), 6.92 (s, 1H), 4.22 (dd, J = 1.6, 5.8 Hz, 1H), 4.41 (m, 1H), 3.92 (s, 3H), 3.36 (m, 1H), 2.03 (dd, J = 3.7, 7.9 Hz, 1H), 1.73 (apparent t, J = 4.2 Hz, 1H), 1.56 (s, 9H); IR (film) ν_{max} 3295, 2919, 1713, 1637, 1542 cm^{-1}; MALDI-HRMS (DHB) *m/z* 695.2242 (M + Na$^+$, $C_{37}H_{32}N_6O_7$ requires *m/z* 695.2225). (+)-(8b*R*, 9a*S*)-**9**: $[\alpha]^{25}_D$ +30 (*c* 0.04, DMF). *ent*-(−)-(8b*S*, 9a*R*)-**9**: $[\alpha]^{25}_D$ −30 (*c* 0.04, DMF).

***N*-(2-(*N*-((2-Methoxycarbonyl)indol-5-yl)carbamoyl)indol-5-yl)-1,2,9,9a-tetrahydrocyclopropa[*c*]pyrido[3,2-*e*]indol-4-one-7-carboxamide (Indole$_2$-CPyI-H, 16).** A sample of **15** (2.0 mg, 2.8 μmol) was treated with 150 μL of 4 N HCl/EtOAc. The yellow reaction mixture was stirred at 25 °C for 30 min and was concentrated under a stream of N_2. The resulting red residue was suspended in 100 μL of THF and treated with 100 μL of saturated aq $NaHCO_3$. The biphasic solution was stirred for 4 h, diluted with H_2O, and extracted with EtOAc. The combined organic phases were concentrated under a stream of N_2 and placed under vacuum to afford **16** (1.3 mg, 81%) as a tan residue: ^{1}H NMR (DMF-d_7, 400 MHz) δ 11.88 (br s, 2H), 10.41 (m, 2H), 9.18 (d, J = 2.1 Hz, 1H), 8.34 (d, J = 2.1 Hz, 1H), 8.30 (s, 1H), 8.15 (d, J = 2.1 Hz, 1H), 7.74 (dd, J = 8.8, 2.1 Hz, 1H), 7.59 (m, 2H), 7.54 (s, 1H), 7.52 (s, 1H), 7.50 (s, 1H), 7.20 (s, 1H), 5.72 (d, J = 1.2 Hz, 1H), 3.90 (s, 4H), 3.70 (d, J = 10.4 Hz, 1H), 3.31 (m, 1H), 1.87 (dd, J = 7.1, 3.3 Hz, 1H), 1.41 (apparent t, J = 4.2 Hz, 1H); IR (film) ν_{max} 3261, 2919, 1702, 1634, 1538 cm^{-1}; MALDI-HRMS (DHB) *m/z* 573.1881 (M + H$^+$, $C_{32}H_{24}N_6O_5$ requires *m/z* 573.1870). (+)-(8b*R*, 9a*S*)-**16**: $[\alpha]^{25}_D$ +14 (*c* 0.065, DMF). *ent*-(−)-(8b*S*, 9a*R*)-**16**: $[\alpha]^{25}_D$ −17 (*c* 0.065, DMF).

***N*-(2-(*N*-((2-Methoxycarbonyl)indol-5-yl)carbamoyl)indol-5-yl)-3-acetyl-5-(benzyloxy)-1-(chloromethyl)-1,2-dihydro-3*H*-pyrido[3,2-*e*]indole-8-carboxamide (17).** A sample of **14** (3.5 mg, 4.4 μmol) was treated with 200 μL of 4 N HCl/EtOAc. The yellow reaction mixture was stirred at 25 °C for 30 min and was concentrated under a stream of N_2. The red residue was dissolved in 100 μL of anhydrous DMF and treated sequentially with $NaHCO_3$ (1.1 mg, 13.1 μmol) and acetyl chloride (0.82 mg, 8.8 μmol). The reaction mixture was stirred for 12 h and diluted with H_2O. The resulting precipitate was collected by centrifugation, washed with H_2O, and dried under reduced pressure to give **17** (2.6 mg, 81%) as a yellow film: ^{1}H NMR (DMF-d_7, 400 MHz) δ 11.89 (d, J = 2.0 Hz, 1H), 11.86 (d, J = 1.2 Hz, 1H), 10.61 (s, 1H), 9.30 (d, J = 2.0 Hz, 1H), 9.03 (d, J = 2.0 Hz, 1H), 8.51 (s, 1H), 8.33 (m, 2H), 7.76 (dd, J = 2.1, 8.8 Hz, 1H), 7.68 (m, 2H), 7.63 (d, J = 1.6 Hz, 1H), 7.59 (d, J = 8.8 Hz, 1H), 7.54 (m, 2H), 7.45 (apparent t, J = 7.1 Hz, 2H), 7.38 (apparent t, J = 7.5 Hz, 1H), 7.20 (d, J = 2.1 Hz, 1H), 5.41 (s, 2H), 4.52 (m, 1H), 4.37 (m, 1H), 4.24 (m, 2H), 4.04 (m, 1H), 3.90 (s, 3H), 2.33 (s, 3H); IR (film) ν_{max} 3283, 2919, 1707, 1654, 1642 cm^{-1}; MALDI-HRMS (DHB) *m/z* 741.2213 (M + H$^+$, $C_{41}H_{33}ClN_6O_6$ requires *m/z* 741.2223). (+)-(1*S*)-**17**: $[\alpha]^{25}_D$ +213 (*c* 0.07, DMF). *ent*-(−)-(1*R*)-**17**: $[\alpha]^{25}_D$ −210 (*c* 0.07, DMF).

***N*-(2-(*N*-((2-Methoxycarbonyl)indol-5-yl)carbamoyl)indol-5-yl)-3-acetyl-1-(chloromethyl)-5-hydroxy-1,2-dihydro-3*H*-pyrido[3,2-*e*]-indole-8-carboxamide (18).** A suspension of **17** (3.0 mg, 4.0 μmol) and 10% Pd−C (3.0 mg, 1 wt equiv) in 200 μL of anhydrous THF was treated with 25% aq HCO_2NH_4 (12.8 mg, 51 μL, 200 μmol, 50 equiv). The reaction mixture was stirred for 5 h and filtered through Celite. The filtrate was concentrated under a stream of N_2 to afford **18** (2.6 mg, 100%) as a light yellow residue: ^{1}H NMR (DMF-d_7, 400 MHz) δ 11.88 (s, 1H), 11.60 (s, 1H), 10.23 (s, 1H), 9.94 (s, 1H), 9.05 (s, 1H), 8.32 (d, J = 2.1 Hz, 2H), 8.18 (d, J = 1.7 Hz, 1H), 7.73 (m, 2H), 7.54 (m, 3H), 7.48 (s, 1H), 7.45 (m, 1H), 7.20 (d, J = 1.7 Hz, 1H), 4.21 (m, 1H), 4.10 (dd, J = 1.0, 9.2 Hz, 1H), 3.95 (m, 1H), 3.90 (s, 3H), 3.72 (m, 2H), 2.18 (s, 3H); IR (film) ν_{max} 3260, 2919, 1695, 1637, 1537 cm^{-1}; MALDI-HRMS (DHB) *m/z* 651.1772 (M + H$^+$, $C_{34}H_{27}ClN_6O_6$ requires *m/z* 651.1753). (−)-(1*S*)-**18**: $[\alpha]^{25}_D$ −11 (*c* 0.14, DMF). *ent*-(+)-(1*R*)-**18**: $[\alpha]^{25}_D$ +9 (*c* 0.14, DMF).

***N*-(2-(*N*-((2-methoxycarbonyl)indol-5-yl)carbamoyl)indol-5-yl)-3-acetyl-1,2,9,9a-tetrahydrocyclopropa[*c*]pyrido[3,2-*e*]-indol-4-one-7-carboxylamide (Indole$_2$-CPyI-Ac, 19).** A sample of **18** (1.4 mg, 2.2 mmol) was suspended in 300 μL of THF and treated with 300 μL of saturated aq $NaHCO_3$. The biphasic solution was stirred for 4 h, diluted with H_2O, and extracted with EtOAc. The combined organic phases were concentrated under a stream of N_2 and placed under vacuum to afford **19** (1.2 mg, 92%) as a tan residue: ^{1}H NMR (DMF-d_7, 400 MHz) δ 11.89 (br s, 2H), 10.52 (br s, 1H), 10.43 (br s, 1H), 9.25 (d, J = 1.7 Hz, 1H), 8.34 (d, J = 1.7 Hz, 2H), 8.28 (d, J = 2.1 Hz, 1H), 7.76 (s, 1H), 7.74 (d, J = 2.1 Hz, 1H), 7.60 (s, 2H), 7.54 (s, 1H), 7.51 (d, J = 6.7 Hz, 1H), 7.20 (s, 1H), 4.31 (m, 2H), 3.90 (s, 3H), 3.38 (m, 1H), 2.30 (s, 3H), 2.02 (dd, J = 3.8, 7.9 Hz, 1H), 1.72 (apparent t, J = 4.6 Hz, 1H); IR (film) ν_{max} 2919, 1701, 1637, 1537, 1231 cm^{-1}; MALDI-HRMS (DHB) *m/z* 615.1991 (M + H$^+$, $C_{34}H_{26}N_6O_6$ requires *m/z* 615.1991). (+)-(8b*R*, 9a*S*)-**19**: $[\alpha]^{25}_D$ +18 (*c* 0.06, DMF). *ent*-(−)-(8b*S*, 9a*R*)-**19**: $[\alpha]^{25}_D$ −20 (*c* 0.05, DMF).

Acknowledgment. We gratefully acknowledge the financial support of the National Institutes of Health (Grant CA41986), The Skaggs Institute for Chemical Biology, and Corixa Pharmaceuticals. S.E.W is a Skaggs Fellow and recipient of an ARCS fellowship. We thank Michael P. Hedrick for conducting the cytotoxic assays.

Supporting Information Available: Experimental details for the DNA alkylation studies, gel figures of (+)-**10**, *ent*-(−)-**10**, and *ent*-(−)-**9** in w836 DNA (Figure S1), gel figures of (+)-**1**, *ent*-(−)-**1**, and (+)-**9**, **16**, and **19** in w794 DNA (Figure S2), a representative gel figure used to establish rates of DNA alkylation (Figure S3), a Table S1 of absolute rate constants, and representative data treatments for establishing rates (Figure S4) (pdf). This material is available free of charge via the Internet at http://pubs.acs.org.

JA010769R